The effects of pH, salt and bond stiffness on charged dendrimers

2010 J. Phys.: Condens. Matter 22 232101

(http://iopscience.iop.org/0953-8984/22/23/232101)

IOP FTC
IOP Publishing
Journal of Physics: Condensed Matter
J. Phys.: Condens. Matter **22** (2010) 232101 (8pp)
doi:10.1088/0953-8984/22/23/232101

FAST TRACK COMMUNICATION

The effects of pH, salt and bond stiffness on charged dendrimers

Sebastian Huißmann[1], **Aaron Wynveen**[1,3], **Christos N Likos**[1,2] **and Ronald Blaak**[1]

[1] Institute of Theoretical Physics, Heinrich Heine University of Düssedorf, Universitätsstraße 1, D-40225 Düsseldorf, Germany
[2] Faculty of Physics, University of Vienna, Sensengasse 8/12, A-1090 Vienna, Austria

E-mail: sebastian@thphy.uni-duesseldorf.de

Received 8 April 2010, in final form 16 April 2010
Published 30 April 2010
Online at stacks.iop.org/JPhysCM/22/232101

Abstract
We have performed molecular dynamics simulations of charged dendrimers with various charge distributions, and including both rigid and soft bonds between the monomers. Whereas the rigid bonds result in a shell-like structure, the soft bonds lead to a larger dendrimer size and a more homogeneous monomer distribution. The measured density profiles of counter-ions and co-ions are compared with those stemming from Poisson–Boltzmann theory. The latter is in very good agreement with simulations for the soft-bond model, whereas for rigid bonds, significant discrepancies arise caused by the fact that Poisson–Boltzmann theory neglects finite-size ion effects. The addition of monovalent salt has no significant influence on the behavior of the dendrimers.

(Some figures in this article are in colour only in the electronic version)

1. Introduction

Dendrimers are macromolecules with a highly and regularly branched internal structure. They have been synthetically prepared since the late 1970s [1] and steady progress has led to efficient synthesis techniques [2]. The abundant freedom in modifying their architecture makes them attractive for numerous technological applications. Previous research activities on neutral dendrimers showed that, due to back-folding of end-groups, they are found in a compact, dense-core conformation even for high generation numbers [3, 4]. The finding of a dense-core conformation has been confirmed by a large number of simulation studies [5, 6], self-consistent field calculations [8], and scattering experiments [9, 10]. Dendrimers are also an interesting model system for colloidal/nanoparticles with a tunable stiffness [11, 12] that can bridge the gap between flexible polymers and rigid spheres.

However, neutral dendrimers only form a restricted subset of all possible architectures. An interesting question is that of how the introduction of charge, e.g., through variation of the pH value of the solution, influences the shape of the dendrimer [13]. Whereas in the case of polyelectrolyte chains and stars in which changing the charge of the constituent atoms induces a transition from coiled to rod-like conformations [14, 15], the charging of dendrimers might also lead to a stretched, open conformation which would allow for the absorption of smaller guest molecules in the 'hollow' host. The addition of salt further influences the screening of the Coulomb interaction between the charged segments, leading to a collapse of the dendrimer for higher valences of salt ions [16, 17]. By means of quantitative SANS data analysis and experiments [18–22, 13] it has been found that the size of the dendrimer is only weakly dependent on changes of the pH, the latter being a direct way to influence the degree of charging of the molecule.

Previous simulation studies [23, 24, 16, 17] focused mainly on changes of pH and salinity for fixed model interactions. Here we will study the effect of bond stiffness under varying pH conditions and salt concentrations on the behavior of dendrimers. We employ MD simulations to show

[3] Present address: School of Physics and Astronomy, University of Minnesota, 116 Church Street SE, Minneapolis, MN 55455, USA.

that softening of the bonds has a huge impact on both size of the dendrimer and its conformational properties. In section 2 we give a short overview of the model and the simulation technique used. In section 3 we describe a theoretical approach used to ascertain the charge distribution of the counter-ions and co-ions around the dendrimer by an application of Poisson–Boltzmann theory. The results are presented in section 4, where we focus on the influence of the pH of the solvent as well as considering the effects of added salt, up to physiological concentrations, on the structure of the dendrimers. We conclude in section 5 with a brief summary and outlook.

2. The simulation model

In order to model the dendrimers, we employ a bead–spring model. A single pair of monomers, generation 0, forms the center of the internal structure of the dendrimer. Successive generations are added by connecting two additional monomers to each site of the highest generation only. A dendrimer thus formed will contain 2^{g+1} monomers in every generation g, whereas G denotes the total number of generations. Here we will focus on a dendrimer of generation $G = 4$, which has a total of 62 monomers.

In order to prevent monomers from coming arbitrarily close, each pair of monomers at a relative distance r interacts via the purely repulsive, truncated and shifted Lennard-Jones potential [25]:

$$V_{\mathrm{LJ}}(r) = \begin{cases} 4\epsilon\left[\left(\frac{\sigma}{r}\right)^{12} - \left(\frac{\sigma}{r}\right)^{6} + \frac{1}{4}\right] & r \leqslant 2^{1/6}\sigma \\ 0 & r > 2^{1/6}\sigma, \end{cases} \quad (1)$$

where the interaction strength ϵ fixes our unit of energy and the monomer diameter σ will be our unit of length. The latter can be identified as the persistence length [26, 27].

The connectivity between monomers is described using the so-called finite extensible nonlinear elastic (FENE) potential:

$$V_{\mathrm{FENE}}(r) = \begin{cases} -U_0\left(\frac{R_0}{\sigma}\right)^2 \ln\left[1 - \left(\frac{r}{R_0}\right)^2\right] & r \leqslant R_0 \\ \infty & r > R_0. \end{cases} \quad (2)$$

Here R_0 is the maximal bond length between two monomers and U_0 is a measure for the spring constant.

In our simulations, we examine two types of bond stiffness: rigid bonds ($U_0 = 15\epsilon$, $R_0 = 1.5\sigma$) and soft bonds ($U_0 = 1\epsilon$, $R_0 = 10\sigma$). The values used for the stiff bonds are realistic and yield excellent agreement between theory and experiment [7]. Softer bonds could be obtained by the introduction of spacers. The resulting bond interactions $V(r) = V_{\mathrm{LJ}}(r) + V_{\mathrm{FENE}}(r)$, including short-range repulsion, for both kinds of bonds are shown in figure 1.

The short-range repulsive interaction between monomers ensures that for dendrimers with rigid bonds the unphysical crossing of bonds does not occur [28]. Such crossings, however, are possible for the soft bonds. Since we will here focus mainly on static quantities, such unphysical movements should not affect the results presented here. Although these bonds are too soft for the microscopic/atomistic scale, and have not yet been employed on the mesoscopic/colloidal scale, they can nevertheless serve as a simple approximation for a short sequence of monomers that acts as spacers between the nodes of the dendrimer.

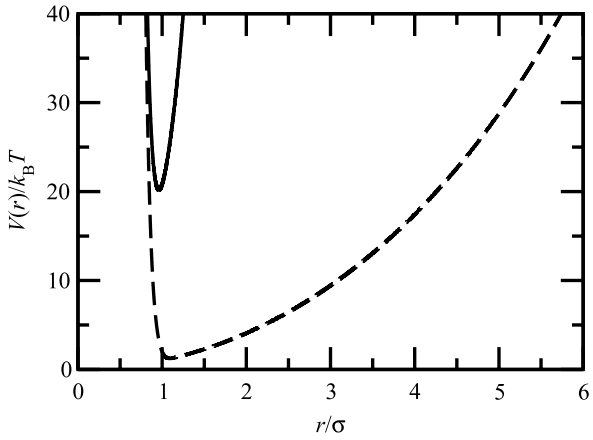

Figure 1. The total interaction potential $V(r)$ for two connected beads within a dendrimer, resulting from the sum of the steric (equation (1)) and bonded (equation (2)) potentials. The potentials for rigid and soft bonds are denoted by the solid and dashed lines, respectively.

The electrostatic interaction between charged monomers is described using the Coulomb potential

$$V_{\mathrm{Coulomb}}(r) = k_{\mathrm{B}}T\lambda_{\mathrm{B}}\frac{Z_i Z_j}{r} \quad (3)$$

with Z_i and Z_j the charge numbers, k_{B} the Boltzmann constant, T the temperature and λ_{B} the Bjerrum length given by

$$\lambda_{\mathrm{B}} = \frac{e^2}{\epsilon_{\mathrm{r}}k_{\mathrm{B}}T}, \quad (4)$$

where ϵ_{r} is the relative permittivity.

For the solvent of our simulations we use implicit water at room temperature, which is modeled by choosing $\epsilon_{\mathrm{r}} = 80$, $\lambda_{\mathrm{B}} = 3\sigma$, and a temperature $k_{\mathrm{B}}T = 1.2\epsilon$, which is maintained via an Andersen thermostat. This results in a particle diameter $\sigma = 0.238$ nm for our unit length. The monomers are chosen to be either neutral or monovalently charged. For charged dendrimers, the counter-ions released by the ionizable groups are included to guarantee overall charge neutrality. All counter-ions and co-ions interact, in addition to their Coulomb interaction, via the same short-range repulsion (1) as the monomers of the dendrimer.

The simulation box was chosen to be cubic in shape with length $L = 60\sigma$. The long-range Coulomb interactions are handled by the Ewald summation method, with the appropriate parameters for the box size and concentrations at hand. Time is measured in units of $\tau = (m\sigma^2\epsilon)^{1/2}$ and up to 5×10^6 and 10^7 time steps of $\delta t = 0.002\tau$ have been used for systems with rigid- and soft-bonded dendrimers, respectively, to gather good statistics. Initial configurations have been allowed to relax for a sufficiently long time to enable the counter-ions to diffuse

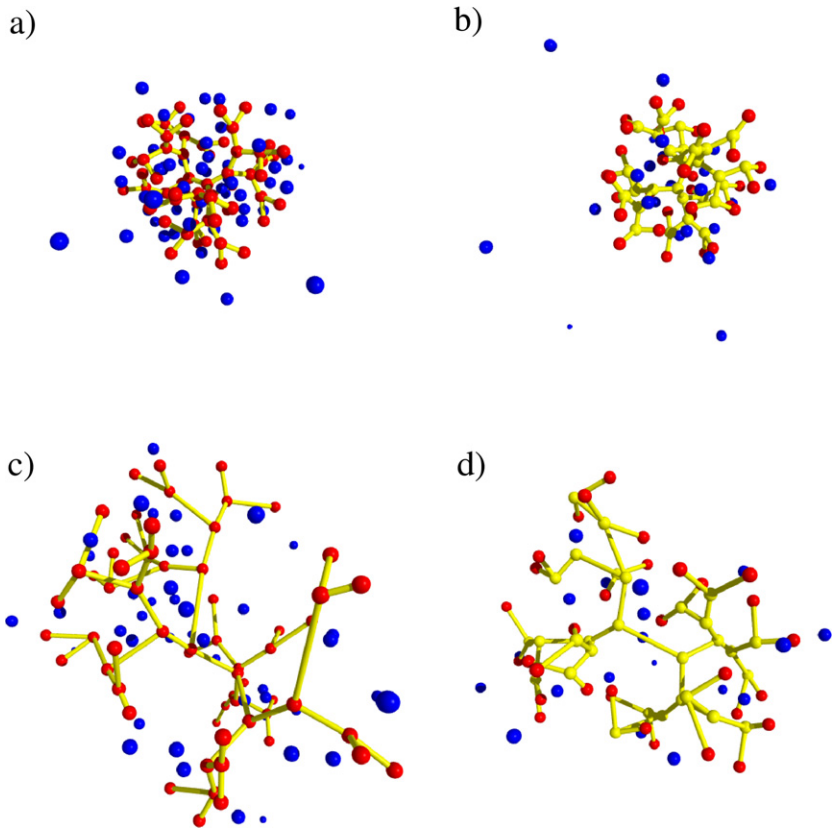

Figure 2. Snapshots from simulation for dendrimers with rigid bonds ((a), (b)) and soft bonds ((c), (d)). The dendrimer types are fully charged, $Z = 62$, in (a) and (c) and only end-group charged, $Z = 32$, in (b) and (d). Neutral monomers are denoted by light gray (yellow), charged monomers by dark (red), and monomer ions by dark (blue), unbonded spheres. All monomers are rendered as spheres with half their Lennard-Jones diameter, for clarity.

into the core of the dendrimer and to reach a steady state for the inward and outward flux.

In our simulation we consider five kinds of dendrimers, which differ only in the way in which they are charged and can be characterized by their total charge number, denoted by Z. In addition to the fully neutral dendrimer with $Z = 0$ as a reference system, we obtain successive types by charging the highest neutral generation available. Therefore the next type $Z = 32$ has only its 32 monomers of the terminal generation charged. If we additionally charge the 16 monomers of generation 3, we obtain the type characterized by $Z = 48$. The next type with $Z = 56$ has all monomers of generations 2, 3, and 4 charged. The last type that we consider is the fully charged dendrimer with $Z = 62$. This process of charging can be realized through a variation of the pH value of the aqueous solution. For instance, the dendrimer can be synthesized in such a way that the monomer units are protonated, and thus charged, at low pH values but remain neutral at high pH values [5]. By the use of appropriate functional groups as monomer units, such as secondary and tertiary amines, only the monomers of the outer generations acquire charges at intermediate pH values. To examine the effect of salt on the behavior of the dendrimers, we have restricted ourselves to monovalent salt at concentrations of 10, 50 and 100 mM, where the corresponding ions were modeled in the same fashion as the counter-ions.

Representative snapshots from the simulations are shown in figure 2, where the difference between the rigid and soft dendrimers is apparent. The effect of the charges in the former case is to reorganize the monomers to minimize electrostatic interactions by maximizing the distances between charged monomers, whereas the size is almost insensitive to pH changes. In the latter case, the soft bonds allow the dendrimer to stretch, which reduces the electrostatic energy in a fashion not available to a dendrimer with rigid bonds, and leads to a more open structure and much more flexibility with respect to internal rearrangements.

3. Theory

Poisson–Boltzmann theory is a tool widely used for analyzing charged, aqueous systems; we will demonstrate here how it may be applied to the dendrimer systems being probed. Results stemming from this method will be compared with simulation results as a check on the simulations and to determine the applicability of such an approach. We calculate the distribution of the counter-ions and co-ions in the solvent around the charged dendrimer by solving the Poisson–Boltzmann equation within a spherical cell of radius $R = (3/(4\pi))^{1/3}L$, i.e., the radius of a sphere whose volume is the system size, L^3, which is given by

$$\nabla^2\psi(r) = -4\pi\lambda_B[Z_m\rho_m(r) + Z_c\rho_c^\infty e^{-Z_c\psi(r)} + Z_{co}\rho_{co}^\infty e^{-Z_{co}\psi(r)}]. \quad (5)$$

Table 1. Radius of gyration R_g measured in units of the monomer diameter σ for rigid and soft bonds in a salt-free solution.

Z	Rigid	Soft
62	2.87	5.6
56	2.81	5.3
48	2.76	5.1
32	2.70	4.8
0	2.51	3.8

Here $\psi(r)$ denotes the dimensionless electrostatic potential as a function of distance r from the center of mass of the dendrimer, ρ_c^∞ and ρ_{co}^∞ are the bulk number densities of counter-ions and co-ions, respectively, and $\rho_m(r)$ is the charge-number density of the dendrimer. The latter gives the radial charge density profile obtained by the simulation that is then used as an input in the equation in order to self-consistently determine the remaining, counter-ion and co-ion, charge density profiles. The charge numbers are $Z_m = Z_{co} = -Z_c = 1$, and the boundary conditions $\nabla\psi(0) = 0$ and $\nabla\psi(R) = 0$ have been applied. The former condition is a result of spherical symmetry, whereas the latter stems from overall charge neutrality of the full cell volume.

The solution to this nonlinear differential equation was obtained by means of the finite-difference method for the salt-free cases. For higher salt concentrations we employed the Gauss–Seidel iteration method [29] using the solutions at lower concentrations as initial guesses.

From the solutions of equation (5) for the electrostatic potentials $\psi(r)$, we obtained the density profiles $\rho_c(r)$ and $\rho_{co}(r)$ for the counter-ions and co-ions, respectively:

$$\rho_c(r) = \rho_c^\infty \exp[-Z_c\psi(r)]; \tag{6}$$

$$\rho_{co}(r) = \rho_{co}^\infty \exp[-Z_{co}\psi(r)]. \tag{7}$$

By integrating the density profiles, we obtain the number of absorbed counter-ions N_{in} as

$$N_{in} = 4\pi \int_0^{R_{max}} dr\, r^2 \rho_c(r), \tag{8}$$

where R_{max} is the maximum distance from the center of mass where the monomers of the dendrimer have been found in simulations.

4. The effect of pH on dendrimers

In this section we will focus on the effect that the pH of the solvent has on the conformational properties of dendrimers. It should be noted, however, that the pH is modeled in an implicit fashion, because we assumed that the change in pH will lead to a change in the overall charge configuration of the dendrimers, as described for the five different cases discussed in section 2. Typically, the isoelectric points of annealed polyelectrolytes are found for a pH in the range 4–5.

A good measure for the typical size of a dendrimer is the radius of gyration R_g, given by

$$R_g^2 = \left\langle \frac{1}{N} \sum_{i=1}^{N} (\mathbf{r}_i - \mathbf{r}_c)^2 \right\rangle \tag{9}$$

Table 2. Average bond length $b(g)$ in units of σ for a monomer in generation g linked with its parent of generation $g-1$ (except for $g = 0$) for the soft-bonded dendrimers.

Z	$b(0)$	$b(1)$	$b(2)$	$b(3)$	$b(4)$
62	2.5	2.3	2.1	2.0	1.7
56	2.4	2.2	2.0	1.9	1.7
48	2.4	2.2	1.9	1.8	1.7
32	2.2	2.1	1.8	1.7	1.6
0	1.8	1.7	1.7	1.6	1.5

where N is the number of monomers and $\mathbf{r}_c$ the center of mass of the dendrimer. The simulation results for varying pH are shown in table 1 for both the soft- and rigid-bonded dendrimers. The short-range Lennard-Jones repulsion models the excluded volume effects present in the neutral dendrimers. Upon charging, the dendrimers swell monotonically, which is mainly due to the electrostatic repulsion between the charged monomers. The increase in size, however, also makes it easier for counter-ions to diffuse within the dendrimer, thus screening the repulsive forces to some extent. The swelling is restricted to about 15% for the fully charged dendrimer compared to the neutral one in the case of rigid bonds. The possibility of stretching the bonds in the soft-bonded dendrimers allows for a significantly larger swelling of almost 50%, which is not surprising considering the shapes of both bond interactions shown in figure 1.

It is clear that the swelling of the overall size of the dendrimers, which can only partially be explained by rearrangement of the monomers within the existing dendrimer structure, needs to be caused by increasing the distances between connected particles. Although all the bond interactions within a dendrimer are the same, the stretching of individual bonds depends on their location within the dendrimer. This can be seen in table 2, where we list the average bond length for the different dendrimer types with soft bonds separated with respect to their generation, i.e., the average bond length $b(g)$ is formed by the connection between a monomer of generation g and its parent of the lower generation $g-1$. The bond $b(0)$ is the single central bond between the two generation 0 monomers. The same observations apply to the bond lengths of the dendrimer types with rigid bonds. However, the changes in bond lengths are very small and are therefore not shown.

It should be noted that the bond stretching observed is not only a direct consequence of the electrostatic repulsion of the particles participating in the bond, but also a collective effect of all repulsive forces in the dendrimer. This is clear from the $Z = 32$ dendrimers for which the central bond $b(0)$ is stretched significantly with respect to the neutral dendrimer, even though only the end-group monomers carry charges. Not only do the bond lengths increase with increasing dendrimer charge, but also the stretching increases with decreasing generation. This is not unexpected, if one realizes that by stretching a single central bond, on average most monomer distances between monomers of different branches are increased, thus diminishing the electrostatic potential. In fact this argument is not restricted to the electrostatic interaction, because even for the neutral dendrimer the stretching of a central bond will be

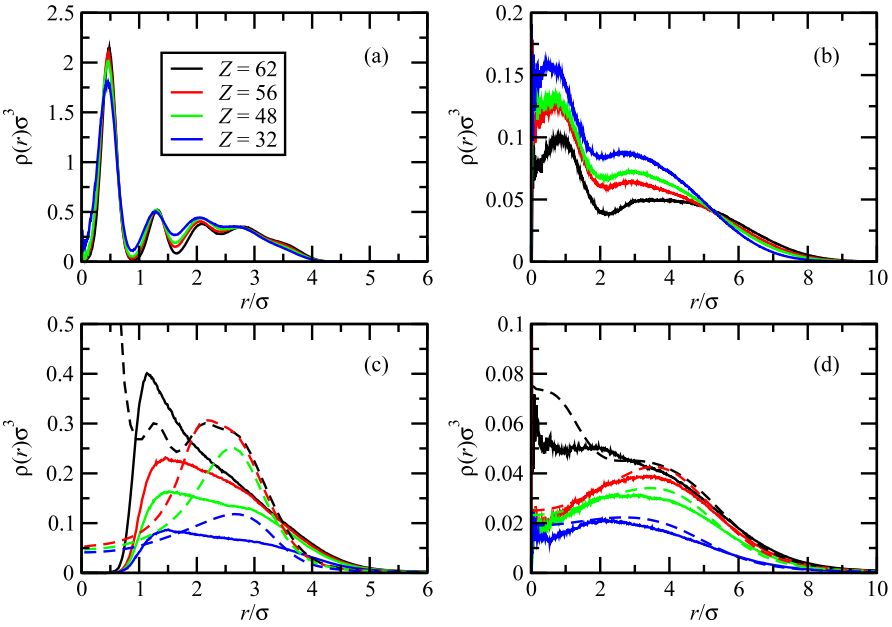

Figure 3. Simulation results for the radial density profiles ((a), (b)) and counter-ion distributions ((c), (d)) at different pH values. Results for dendrimers with rigid bonds are shown in panels (a), (c) whereas those for soft-bonded dendrimers appear in panels (b), (d). The counter-ion distributions obtained by Poisson–Boltzmann theory are shown as dashed lines.

beneficial for the short-range repulsive forces and, at the cost of a somewhat higher energy, will increase the entropic freedom.

A better understanding of the internal structure is offered by the radial density profiles $\rho(r)$ measured with respect to the center of mass $\mathbf{r}_c$,

$$\rho(r) = \left\langle \sum_{i=1}^{N} \delta(\mathbf{r} - \mathbf{r}_i + \mathbf{r}_c) \right\rangle, \tag{10}$$

where $\mathbf{r}_i$ denotes the position of the ith monomer within the dendrimer or, alternatively, could denote the positions of counter-ions or co-ions.

Figure 3 shows the radial density profiles for the monomers and the counter-ion distributions for both cases of rigid- and soft-bonded dendrimers. Upon charging, the dendrimers swell due to electrostatic repulsion between the charged monomers. In combination with the connectivity of the monomers, this results in a clear shell-like density profile in the case of rigid bonds, whereas the additional freedom of bond stretching for the soft-bonded dendrimers leads to a less structured density profile. The space within the dendrimer that has been freed by the swelling becomes partially occupied by the counter-ions, which can easily diffuse into the core of the dendrimer. This effect is obviously enhanced by an increased overall charge of the dendrimer. Whereas the additional freedom in arranging monomers in the soft-bonded dendrimers due to bond stretching allows the counter-ions to occupy the space throughout the dendrimer, the shell structure maintained by the rigid bonds expels them via the short-range repulsive Lennard-Jones forces from the center of the dendrimer.

The results for the counter-ion distributions from the Poisson–Boltzmann approach based on the measured radial density profiles are also shown in figures 3(c) and (d). In the case of the soft bonds, this leads to a remarkably good agreement with simulation results. In contrast, for the rigid-bonded dendrimers, there is a significant discrepancy. This is caused by the fact that the Poisson–Boltzmann theory neglects the steric interactions that, in particular for the rigid-bonded dendrimer, expel the counter-ions from the region close to the center of mass, which in the shell-like structure of the dendrimer lies close to the central monomer pair on average. For the dendrimer with soft bonds, the radial density profiles are much less structured, which does not require the near coincidence of the center of mass and the center of the dendrimer, i.e., the location of the $g = 0$ generation. Only in the case of the fully charged dendrimer does the Coulomb attraction of the central monomers lead to a significant deviation in the core region.

The existence of the shell structure of the dendrimer in the rigid-bonded case, and its absence in the soft-bonded dendrimers, is illustrated in figure 4, where the contributions to the radial density profiles of the individual generations are shown for dendrimers with only the terminal generation charged. The mutual repulsion of the monomers and restricted bond lengths for the rigid dendrimers push the monomers of the last generation further outwards, enforcing a shell-like structure on the monomers of lower generation, with almost no back-folding present. For the dendrimer with soft bonds, the flexibility gained by stretching not only leads to a much larger size, but also enables the charged monomers to distribute over the whole available space occupied by the dendrimer; it is even possible for them to be found in the core region. The same is true for the monomers of lower generations, with the exception of the central ones, which by construction are close to the center of mass.

In table 3 we list the number N_{in} of absorbed counter-ions as obtained from simulation and theory. Hereby, a counter-ion is assumed to be absorbed if its distance to the center

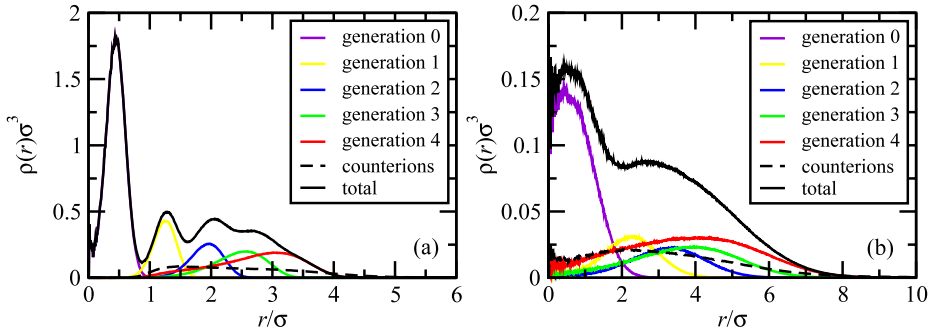

Figure 4. Radial density profiles of the monomers of end-group charged dendrimers: (a) in the rigid bonds; (b) in the soft bonds. Also shown is a breakdown in the contributions emerging from each different generation. Partial generation densities are shown in the order of growing generation number from left to right.

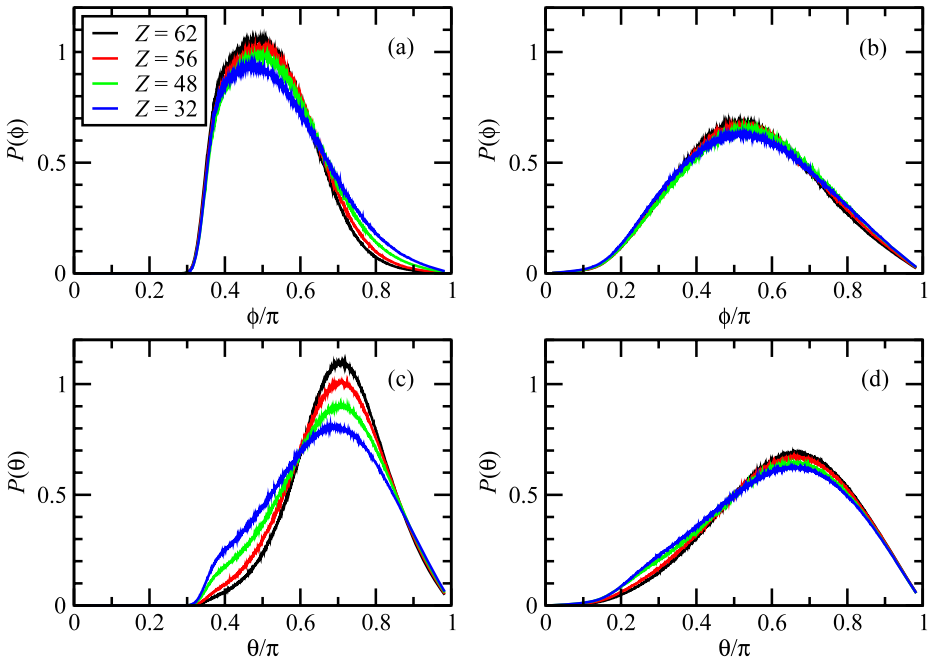

Figure 5. Probability distributions of the angles ϕ and θ for all kinds of dendrimers considered in this work. Panels (a) and (c) show results pertaining to rigid-bonded dendrimers, whereas panels (b) and (d) demonstrate the results for soft-bonded ones.

Table 3. The number of absorbed counter-ions N_{in} for the salt-free solutions from simulation (sim) and Poisson–Boltzmann theory (th).

	Rigid		Soft	
Z	$N_{\text{in}}^{(\text{sim})}$	$N_{\text{in}}^{(\text{th})}$	$N_{\text{in}}^{(\text{sim})}$	$N_{\text{in}}^{(\text{th})}$
62	46	50	46	46
56	40	44	40	42
48	32	36	33	34
32	18	21	18	19

of mass of the dendrimer is less than the maximum distance R_{max} at which a monomer of that dendrimer is found within the simulations. In the case of the rigid-bonded dendrimers this value $R_{\text{max}} = 4.7\sigma$ is the same for the different kinds of charge distributions, whereas for the soft-bonded dendrimers this increases somewhat with the overall charge and ranges from $R_{\text{max}} = 11\sigma$ to 13σ. Not surprisingly, this number increases with the overall charge Z of the dendrimer but seems to be insensitive to the nature of the bonds. Since the Poisson–Boltzmann theory neglects the steric interactions due to the short-range Lennard-Jones repulsion between monomers, it overestimates the number of absorbed counter-ions. Since, in the case of the rigid bonds, the charged monomers are forced to remain in a smaller enclosed volume, this overestimation is further enhanced.

A way to characterize the internal freedom in the conformation of the dendrimer is to measure the bond angles θ and ϕ averaged over each node. Here θ, associated with a monomer of generation g, is defined as the bond angle between the bond with the joined monomer of the lower generation $g - 1$ and those of each of the joined monomers of the higher generation $g + 1$. Likewise, ϕ, associated with the same monomer of generation g, is defined as the bond angle between the two bonds to both linked monomers of the higher generation $g + 1$. The probability distributions of the bond

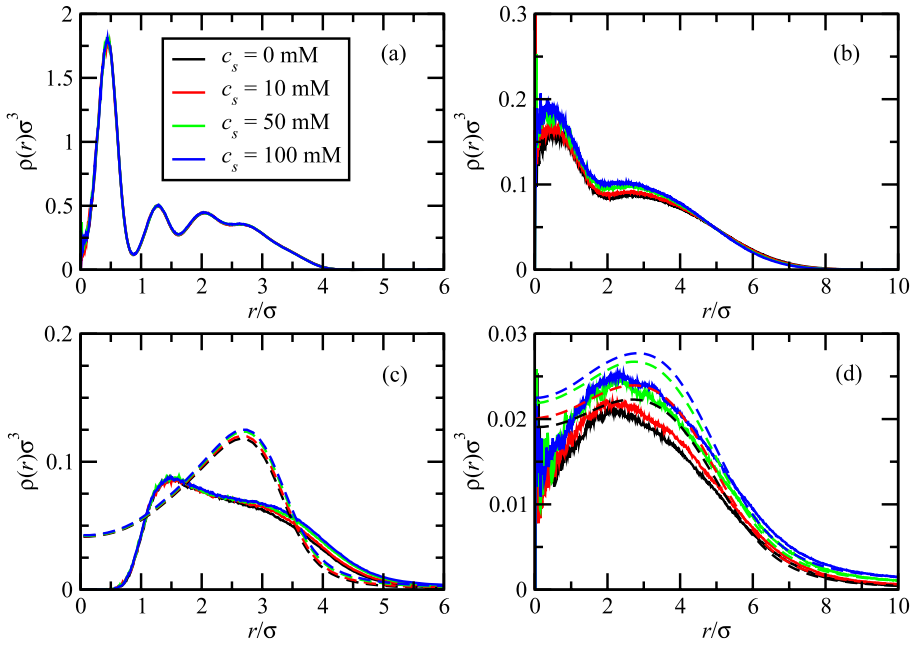

Figure 6. Radial density profiles for terminal-group charged (a) rigid and (b) soft dendrimers at varying salt concentrations ranging between 0 and 100 mM. The corresponding counter-ion distributions are shown in panels (c) and (d), respectively. Solid lines: simulations; dashed lines: Poisson–Boltzmann theory. Salt concentrations, as indicated in the legend, decrease from top to bottom.

Table 4. The radius of gyration R_g and the number of absorbed counter-ions N_{in} from simulation (sim) and Poisson–Boltzmann (th) for different salt concentrations c_s. Results are provided, again, for a dendrimer with only the end-groups charged and with either rigid or soft bonds.

	Rigid bonds			Soft bonds		
c_s (mM)	R_g/σ	$N_{in}^{(sim)}$	$N_{in}^{(th)}$	R_g/σ	$N_{in}^{(sim)}$	$N_{in}^{(th)}$
0	2.70	18	21	4.8	18	19
10	2.70	19	22	4.7	20	21
50	2.70	20	23	4.6	24	25
100	2.69	20	24	4.6	27	28

angles are shown in figure 5. The steric interactions in the rigid case result in a vanishing of the probability for values of bond angles smaller than $\pi/3$ (figures 5(a) and (c)). Upon increasing the charge of the dendrimer, this effect becomes less important, since the repulsive Coulomb interactions lead to a natural avoidance of small angles. In the soft-bonded dendrimers, the steric restriction can be bypassed by exploiting the fact that bonds can be stretched, thus allowing for even small angles because of the increased distance between joined monomers. This also causes the angle distributions to be less sensitive to the overall charge of the dendrimer.

For star polymers, it is known that an increase of the salinity of the solution can result in a dramatic collapse of the polymers [15]. In order to investigate whether a similar behavior can be observed for dendrimers, we performed simulations at three different salt concentrations of monovalent ions. Hereby, we focus on the dendrimers with only the terminal groups charged ($Z = 32$) and both kinds of bonds. For the salinity we chose physiologically relevant concentrations of 10, 50, and 100 mM.

The resulting density profiles are shown in figure 6 and indicate that, at least for monovalent salt ions, addition of salt at these concentrations has no significant effect on the conformation of the rigid-bonded dendrimers. In the case of the soft-bonded ones, it results in a slightly more compact structure as indicated by change in the radius of gyration in table 4. This is due to a minor increase in the counter-ion concentration within the dendrimer, which increasingly screens the Coulombic repulsion between the charged dendrimer monomers. At the same time the number of absorbed co-ions, where the same criterion as for the counter-ions is used, for all dendrimers and concentrations remains less than 1. As mentioned before, the results from a Poisson–Boltzmann calculation for the rigid dendrimers are somewhat inaccurate, since it neglects the short-range repulsive steric interactions between monomers and ions, which are amplified in the central region of the rigid-bonded dendrimer. For the soft-bonded dendrimers, a similar, but smaller, discrepancy can be seen as well. In the outer regions and outside the dendrimer, however, Poisson–Boltzmann theory predicts density profiles for counter-ions and co-ions that agree quite well with the simulation data as illustrated in figure 7.

5. Summary and conclusions

We have performed molecular dynamic simulations of charged dendrimers of generation 4. In experiments the overall charge can be handled by modifying the pH of the solvent, and the location of the chargeable groups can be controlled by the appropriate synthesis techniques. We have restricted these investigations, for simplicity, to four different kinds of charge distributions, starting from ones with only chargeable end-groups, to the fully charged dendrimer by successively

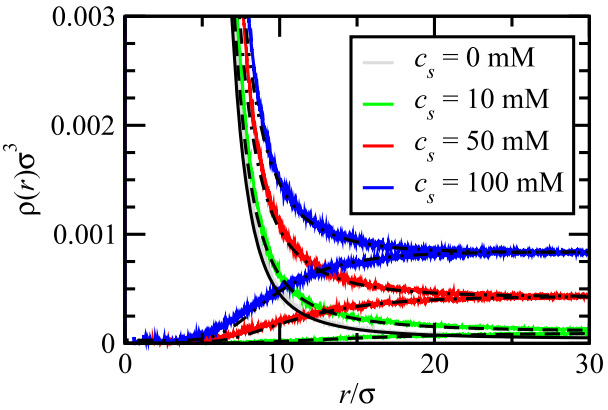

Figure 7. A comparison of the simulation data and Poisson–Boltzmann results for the counter-ion and co-ion distribution for the soft, end-group charged dendrimers at the various salt concentrations. The colored lines denote simulation results for the salt concentrations indicated in the legends, whereas the black lines illustrate results from Poisson–Boltzmann theory. For the case of no salt ($c_s = 0$ mM), there is a single curve corresponding to the counter-ions, whereas for finite salt concentrations the monotonically decreasing curves denote counter-ion profiles and the increasing ones those of the co-ions.

adding charge to lower generation monomers. In order to investigate the effect of the bond stiffness on the behavior of the dendrimers, we also considered two different varieties: the rigid bonds, which almost keep the bond length fixed, and a soft bond that can be stretched up to almost twice its optimal length.

The Coulomb repulsion of the charged monomers results in an increasing size of the dendrimer of about 10% for our rigid parameters, but almost 50% for the weaker bonds. However, whereas in the rigid case the dendrimer forms a shell-like structure for its monomers of different generations, in the case of the soft bonds the additional stretching allows for a more homogeneous distribution of the monomers and back-folding. The charged monomers draw counter-ions into the dendrimer, compensating roughly 60%–70% of the overall charge of the dendrimer. The size of the simulation box is here already sufficiently large to guarantee that this number does not change substantially with increasing box size.

The distribution profiles of the counter-ions obtained by the simulations have been compared with predictions of a Poisson–Boltzmann theory based on the monomer profiles from the simulations. For the soft-bonded dendrimers this results in an excellent agreement. For the dendrimers with rigid bonds, however, a significant discrepancy arises, which can be explained by the fact that this theory neglects the short-range repulsive interactions between monomers and counter-ions. Due to the shell-like structure, the central monomer pair on average will be close to the center of mass of the whole dendrimer, thus expelling counter-ions from the core region despite the Coulomb attraction of the counter-ions to the core in the fully charged dendrimers.

The addition of monovalent salt of various concentrations has no substantial effect on the behavior of the dendrimers. It results in a minor increase in size and number of absorbed counter-ions. It is to be expected, however, that the addition of multivalent salt will lead to a collapse similar to that found for polyelectrolyte stars, but this falls outside the scope of the current work and is left for future studies. Finally, future work will address the question of the effect of pH and salinity of the solvent on the effective interaction between the different dendrimer types. We expect a Gaussian effective interaction potential with stronger repulsion upon charging, where the range of the interaction can be reduced by increasing the salinity of the solvent.

Acknowledgment

AW has been supported by the Alexander von Humboldt Foundation through a Research Fellowship.

References

[1] Buhleier G E, Wehner W and Vögtle F 1978 *Synthesis* **2** 155
[2] Antoni P, Nystrom D, Hawker C J, Hult A and Malkoch M 2007 *Chem. Commun.* **22** 2249
[3] Götze I O and Likos C N 2003 *Macromolecules* **36** 8189
[4] Rathgeber S, Monkenbusch M, Kreitschmann M, Urban V and Brulet A J 2002 *J. Chem. Phys.* **117** 4047
[5] Ballauff M and Likos C N 2004 *Angew. Chem. Int. Edn* **43** 2998
[6] Likos C N 2006 *Soft Matter* **2** 478
[7] Harreis H, Likos C N and Ballauff M 2003 *J. Chem. Phys.* **118** 1979
[8] Zook T C and Pickett G 2003 *Phys. Rev. Lett.* **90** 015502
[9] Pötschke D, Ballauff M, Lindner P, Fischer M and Vögtle F 1999 *Macromolecules* **32** 4079
[10] Pötschke D, Ballauff M, Lindner P, Fischer M and Vögtle F 2000 *Macromol. Chem. Phys.* **201** 330
[11] Likos C N, Rosenfeldt S, Dingenouts N, Ballauff M, Lindner P, Werner N and Vögtle F J 2002 *Macromol. Chem. Phys.* **203** 1995–2004
[12] Götze I O, Harreis H M and Likos C N 2004 *J. Chem. Phys.* **120** 7761
[13] Nisato G, Ivkov R and Amis E J 2000 *Macromolecules* **33** 4172
[14] Jusufi A, Likos C N and Löwen H 2002 *Phys. Rev. Lett.* **88** 018301
[15] Jusufi A and Likos C N 2009 *Rev. Mod. Phys.* **81** 1753
[16] Tian W and Ma Y 2009 *J. Phys. Chem.* B **113** 13161
[17] Tian W and Ma Y 2010 *Soft Matter* **6** 1308
[18] Liu Y, Porcar L, Hong K, Shew C Y, Li X, Liu E, Butler P D, Herwig K W, Smith G S and Chen W R 2010 *J. Chem. Phys.* **132** 124901
[19] Porcar L, Liu Y, Verduzco R, Hong K, Butler P D, Magid L J, Smith G S and Chen W R 2008 *J. Phys. Chem.* B **112** 14772
[20] Porcar L, Hong K, Butler P D, Herwig K W, Smith G S, Liu Y and Chen W R 2010 *J. Phys. Chem.* B **114** 1751
[21] Chen W R, Porcar L, Liu Y, Butler P D and Magid L J 2007 *Macromolecules* **40** 5887
[22] Li T K, Hong K, Porcar L, Verduzco R, Butler P D, Smith G S, Liu Y and Chen W R 2008 *Macromolecules* **41** 8916
[23] Guipponi G, Buzza D M and Adolf D B 2007 *Macromolecules* **40** 5959
[24] Blaak R, Lehmann S and Likos C N 2008 *Macromolecules* **41** 4452
[25] Weeks J, Chandler D and Andersen H 1971 *J. Chem. Phys.* **54** 5237
[26] des Cloizeaux J and Jannink G 1990 *Polymers in Solution* (Oxford: Clarendon)
[27] Likos C N 2001 *Phys. Rep.* **348** 261
[28] Grest G S and Kremer K 1986 *Phys. Rev.* A **33** 3628
[29] Jackson J D 1999 *Classical Electrodynamics* 3rd edn (New York: Wiley)